balt6/zns-neusci/zns-neusci/zns-orig/zns3079-07a | simmsl | S=3 | 3/6/07 | 10:41 | Art: 3203943 | Input-YY(v)

Development/Plasticity/Repair

Robo1 and Robo2 Cooperate to Control the Guidance of Major Axonal Tracts in the Mammalian Forebrain

Guillermina López-Bendito,[1] Nuria Flames,[1] Le Ma,[2] Coralie Fouquet,[3,4] Thomas Di Meglio,[3,4] Alain Chedotal,[3,4] Marc Tessier-Lavigne,[2,5] and Oscar Marín[1]

[1]Instituto de Neurociencias de Alicante, Consejo Superior de Investigaciones Científicas and Universidad Miguel Hernández, 03550 Sant Joan d'Alacant, Spain, [2]Howard Hughes Medical Institute, Department of Biological Sciences, Stanford University, Stanford, California 94305, [3]Centre National de la Recherche Scientifique, Unité Mixte de Recherche (UMR) 7102, and [4]Université Pierre et Marie Curie–Paris 6, UMR 7102, 75005 Paris, France, and [5]Genentech, Inc., South San Francisco, California 84080

The function of the nervous system depends on the precision of axon wiring during development. Previous studies have demonstrated that Slits, a family of secreted chemorepellent proteins, are crucial for the proper development of several major forebrain tracts. Mice deficient in Slit2 or, even more so, in both Slit1 and Slit2 have defects in multiple axonal pathways, including corticofugal, thalamocortical, and callosal connections. In the spinal cord, members of the Robo family of proteins help mediate the function of Slits, but the relative contribution of these receptors to the guidance of forebrain projections remains to be determined. In the present study, we addressed the function of Robo1 and Robo2 in the guidance of forebrain projections by analyzing *Robo1*-, *Robo2*-, and *Robo1;Robo2*-deficient mice. Mice deficient in Robo2 and, more dramatically, in both Robo1 and Robo2, display prominent axon guidance errors in the development of corticofugal, thalamocortical, and corticocortical callosal connections. Our results demonstrate that Robo1 and Robo2 mostly cooperate to mediate the function of Slit proteins in guiding the major forebrain projections.

Key words: **axon guidance; cortex; repulsion; Robo; Slit; midline; thalamocortical**

Introduction

The development of the major axonal projections in the mammalian forebrain has been extensively studied in the recent years (for review, see López-Bendito and Molnár, 2003; Richards et al., 2004; Price et al., 2006). Among them, the reciprocal connections between the cortex and the thalamus, corticocortical projections linking both cerebral hemispheres through the corpus callosum, and corticofugal projections directed toward the mesencephalon, pons, and spinal cord have received much attention. These connections underlie some of the most essential functions of the mammalian cerebral cortex, such as perception and motor behavior.

Several guidance molecules have been shown to influence the development of these major forebrain connections. For example, Netrin1 is required for the formation of the corpus callosum (Serafini et al., 1996), and it has also been shown to influence the development of corticofugal (Métin et al., 1997; Richards et al., 1997) and thalamocortical projections (Braisted et al., 2000). Similarly, EphA/ephrinA signaling appears to underlie the topographic organization of thalamocortical projections (Dufour et al., 2003; Torii and Levitt, 2005). In addition, Slits have been shown to play a fundamental role in the guidance of all three major forebrain connections (corticocortical, corticofugal, and thalamocortical) in the mammalian forebrain (Bagri et al., 2002).

Slit proteins have been implicated in axon guidance of insects, nematodes, and vertebrates, contributing through different mechanisms to the development of multiple axonal projections. In addition to playing a major role in regulating axon crossing at the midline (Kidd et al., 1999; Long et al., 2004), Slits specify the lateral and dorsoventral positioning of longitudinal axonal pathways (Rajagopalan et al., 2000; Simpson et al., 2000; Bagri et al., 2002; Nguyen Ba-Charvet et al., 2002; Long et al., 2004) and contribute to the formation of commissures by channeling axons into particular regions (Bagri et al., 2002; Hutson and Chien, 2002; Plump et al., 2002; Shu et al., 2003).

As in *Drosophila* (Kidd et al., 1999) and *Caenorhabditis elegans* (Hao et al., 2001), the function of Slit proteins in the vertebrate nervous system is primarily mediated by Robo receptors (Brose et al., 1999; Li et al., 1999; Yuan et al., 1999; Hutson and Chien, 2002; Long et al., 2004; Sabatier et al., 2004). In the mammalian spinal cord, Robo1, Robo2, and the Robo family protein Rig1/Robo3 cooperate to mediate the function of Slit proteins in the

Received Oct. 24, 2006; revised Feb. 15, 2007; accepted Feb. 19, 2007.

This work was supported by grants from Spanish Government (BFU2005-04773/BMC) and the European Young Investigator (EURYI) program (O.M.) and from Association pour la Recherche sur le Cancer (A.C.). G.L.-B. is a "Ramón y Cajal" Investigator from the Consejo Superior de Investigaciones Científicas. N.F. was supported by a Formación de Profesorado Universitario fellowship from the Spanish Ministry of Education. O.M. is a European Molecular Biology Organization Young Investigator, a National Alliance for Research in Schizophrenia and Depression Young Investigator and a EURYI Awardee. We thank M. Pérez for excellence technical assistance, T. Gil and M. Bonete for daily technical support in the laboratory, and Fujio Murakami for Robo1 and Robo2 antibodies. We also thank members from the Marín and Rico laboratories for useful discussions and comments.

Correspondence should be addressed to Dr. Oscar Marín, Instituto de Neurociencias de Alicante, Consejo Superior de Investigaciones Científicas and Universidad Miguel Hernández, 03550 Sant Joan d'Alacant, Spain. E-mail: o.marin@umh.es.

L. Ma's present address: Department of Cell and Neurobiology, Zilkha Neurogenetic Institute, Keck School of Medicine, University of Southern California, Los Angeles, CA 90089.

DOI:10.1523/JNEUROSCI.4605-06.2007

 0270-6474/07/270001-●$15.00/0

balt6/zns-neusci/zns-neusci/zns-orig/zns3079-07a | simmsl | S=3 | 3/6/07 | 10:41 | Art: 3203943 | Input-YY(v)

guidance of commissural axons (Long et al., 2004; Sabatier et al., 2004). In the developing forebrain, the expression pattern of Robo1 and Robo2 strongly suggest their involvement in the guidance of corticocortical, corticothalamic, and corticofugal projections (Marillat et al., 2001; Bagri et al., 2002; Whitford et al., 2002; Sundaresan et al., 2004). Accordingly, a recent study has shown that Robo1 plays a role in the development of some of these pathways, most notably in the formation of corticocortical callosal projections (Andrews et al., 2006).

Here, we investigated the function of Robo1 and Robo2 in the formation of forebrain connections by analyzing mice carrying severe loss-of-function alleles for Robo1, Robo2, or both Robo1 and Robo2 receptors. Our results demonstrate that Robo1 and Robo2 mostly cooperate to control the development of the major axonal tracts in the mammalian forebrain. The resemblance of the axonal defects found in *Robo1;Robo2* and *Slit1;Slit2* double mutants strongly suggests that Robo1 and Robo2 mediate the function of Slit1 and Slit2 in the formation of these connections.

Materials and Methods

Animals. Mice were treated according to protocols approved by the Committee on Animal Research at the University Miguel Hernández, following Spanish and European Union regulations. Embryonic day 13.5 (E13.5), E14.5, and E18.5 embryos were obtained by mating *Robo1*$^{+/-}$, *Robo2*$^{+/-}$, or *Robo1*$^{+/-}$;*Robo2*$^{+/-}$ mice, which were maintained in CD1, C57BL/6, and mixed CD1–C57BL/6 backgrounds, respectively. Genotyping was performed by PCR as described previously (Grieshammer et al., 2004; Long et al., 2004). Because the *Robo1* and *Robo2* genes are linked (being separated by only 1.8 Mb), the *Robo1*$^{+/-}$;*Robo2*$^{+/-}$ colony was generated through meiotic recombination of the mutant alleles (Z. Chen et al., unpublished observations). AQ: D

Immunohistochemistry and in situ *hybridization.* Embryos were obtained by cesarean section, anesthetized by cooling, perfused with 4% paraformaldehyde (PFA) in PBS, and postfixed in PFA for 2–8 h. After postfixation, brains were cryoprotected in 30% sucrose and either frozen in embedding medium and cut in a cryostat [embryonic day 13.5 (E13.5) and E14.5] or frozen and cut in a freezing sliding microtome (E16.5 and E18.5). Immunohistochemistry was performed on 40-μm-thick free-floating sections (E16.5 and E18.5) or on 20-μm-thick cryostat sections mounted onto glass slides (E13.5 and E14.5). Free-floating sections were preincubated in 5% normal serum of the species in which the secondary antibody was raised, 1% BSA, and 0.3% Triton X-100 in PBS for 1 h at room temperature, and subsequently incubated with the primary antiserum for 24–36 h at 4°C in 2% normal serum and 0.3% Triton X-100 in PBS. The following antibodies were used: rabbit polyclonal antibody against Robo1 (kindly provided by Fujio Murakami; diluted 1:1000), rabbit polyclonal antibody against Robo2 (kindly provided by Fujio Murakami; diluted 1:1000), rat polyclonal antibody against L1 (Chemicon, Temecula, CA; diluted 1:200), rabbit anti-green fluorescent protein (Invitrogen, San Diego, CA; 1:1000), rabbit anti-calbindin (Swant, Bellinzona, Switzerland; 1:5000), rabbit anti-calretinin (Chemicon; 1:5000), and rabbit anti-Neuropeptide Y (NPY) (DiaSorin, Stillwater, MN; 1:3000). Sections were then incubated in biotinylated secondary antibodies (Vector Laboratories, Burlingame, CA; 1:200), and then transferred into avidin–biotin–peroxidase complex (ABC kit; Vector Laboratories; 1:200) for 2 h at room temperature. Peroxidase enzyme activity was revealed using 3,3′-diaminobenzidine tetrahydrochloride [0.05% in phosphate buffer (PB), pH 7.4] as chromogen and 0.01% H_2O_2 as substrate. Sections were rinsed, dehydrated and mounted in Eukitt mounting media (Electron Microscopy Sciences, Fort Washington, PA). In each experiment, sections from homozygous mutants and their wild-type and heterozygous littermates were processed together. In control experiments, the primary antibody was replaced by 0.2% Triton X-100 in PB, and then reacted as above. These control sections showed no positive immunoreactivity. Photomicrographs were prepared by light microscopy and documented using a Leica (Nussloch, Germany) DC 500 digital camera. Immunohistochemistry was performed on cryostat sections on glass slides using essentially the same protocol. In some cases, immunofluorescence labeling using fluorochrome-conjugated secondary antibodies was performed on 40 μm free-floating sections. DNA counterstaining was performed with bis-benzimide (2.5 μg/ml in PBS; Invitrogen), and the slides were mounted using Prolong Antifade (Invitrogen). For *in situ* hybridization, 20-μm-thick cryostat sections were hybridized with digoxigenin-labeled probes essentially as described previously (Schaeren-Wiemers and Gerfin-Moser, 1993), using cDNA probes for Robo1 and Robo2 (Bagri et al., 2002). AQ: I

Slit-alkaline phosphatase binding. Human LRR2-Slit1-alkaline phosphatase (AP), human LRR2-Slit2–AP, or control AP constructs were transfected in COS cells. After 2 d, the conditioned media were concentrated and used directly for binding assays as described previously (Kolodkin et al., 1997). Briefly, 20 μm cryostat sections from wild-type, *Robo1*$^{-/-}$, *Robo2*$^{-/-}$, and *Robo1;Robo2* double-mutant brains were fixed 8 min in cooled 100% methanol. After that, sections were washed in 1× PBS, 4 mM $MgCl_2$, and incubated in a blocking solution (1× PBS, 4 mM $MgCl_2$, 10% FBS) for 1 h at room temperature. For the binding step, Slit–AP fusion proteins were diluted from 1/5 to 1/10 in 1× PBS and incubated for 2 h at room temperature. After washes in 1× PBS, 4 mM $MgCl_2$, the bound ligand was fixed to sections with a solution containing 60% acetone, 4% paraformaldehyde, and 20 mM HEPES, pH 7.0. Then, sections were treated at 65°C for 2 h in 1× PBS to inactivate endogenous phosphatases. Finally, the slices were incubated in revelation buffer (100 mM Tris, pH 9.5, 100 mM NaCl, 5 mM $MgCl_2$, 300 mg/ml nitroblue tetrazolium, and 250 mg/ml 5-bromo-4-chloro-3-indolyl phosphate) for 2 h at room temperature. AQ: J

Quantification of axonal length. Neocortical and dorsal thalamic explants were dissected from E17.5 and E13.5 wild-type mice, respectively, and cultured in collagen for up to 96 h. Explants were confronted with COS cells aggregates transfected with *dsRed* or cotransfected with *Slit2* and *dsRed*. After fixation, dorsal thalamus explants were subdivided into four sectors and the length of the 13 longest axons was measured in every explant using SigmaScan Pro software.

Axon tracing. Axon tracing was performed on E14.5 and E18.5 mouse brains after perfusion. Brains were then postfixed by overnight immersion in 4% PFA at 4°C. For neocortical injections, large crystals of 1,1′-dioctadecyl 3,3,3′3′-tetramethylindocarbocyanine perchlorate (DiI) (Invitrogen) were placed into the parietal cortex of E14.5 and E18.5 brains. For dorsal thalamic injections, the brains were bisected into hemispheres, each of which was used for a separate experiment. Small crystals of DiI (0.1–0.3 mm diameter) were injected into the medial face of dorsal thalamus with an insect pin. The depth to which the crystal was inserted into the thalamus or the cortex was ~0.5–1 mm from the midline. The brains were then incubated in 4% PFA for 2–4 weeks at 37°C, rinsed in 0.1 M PB, pH 7.4, and embedded in 4% low-melt agarose. Fifty- to 100-μm-thick sections were then cut on a vibratome (Leica VT 1000S) in the coronal plane and subsequently counterstained with bis-benzimide, coverslipped with Aquamount (BDH, Poole, UK), and photographed in a fluorescence microscope equipped with a Leica DC500 digital camera.

Results

Expression of Robo1 and Robo2 receptors in the developing forebrain

To investigate the role of Robo receptors in axon guidance in the forebrain, we first analyzed their expression pattern focusing on regions and developmental stages where the major axonal tracts navigate and develop. Consistent with previous studies (Marillat et al., 2001; Bagri et al., 2002; Whitford et al., 2002; Sundaresan et al., 2004), *Robo1* and *Robo2* mRNA are highly expressed in the dorsal thalamus and the cerebral cortex at the time when corticofugal and thalamocortical projections form (Fig. 1*A*,*D*). Interestingly, the pattern of expression of *Robo1* and *Robo2* mRNA appears mostly complementary, both in the developing cortex (Fig. 1*B*,*E*) and dorsal thalamus (Fig. 1*C*,*F*). Specifically, cells at the intermediate zone of the developing cortex appear to express *Robo2* (Fig. 1*E*), whereas neurons that begin to accumulate in the F1

balt6/zns-neusci/zns-neusci/zns-orig/zns3079-07a | simmsl | S=3 | 3/6/07 | 10:41 | Art: 3203943 | Input-YY(v)

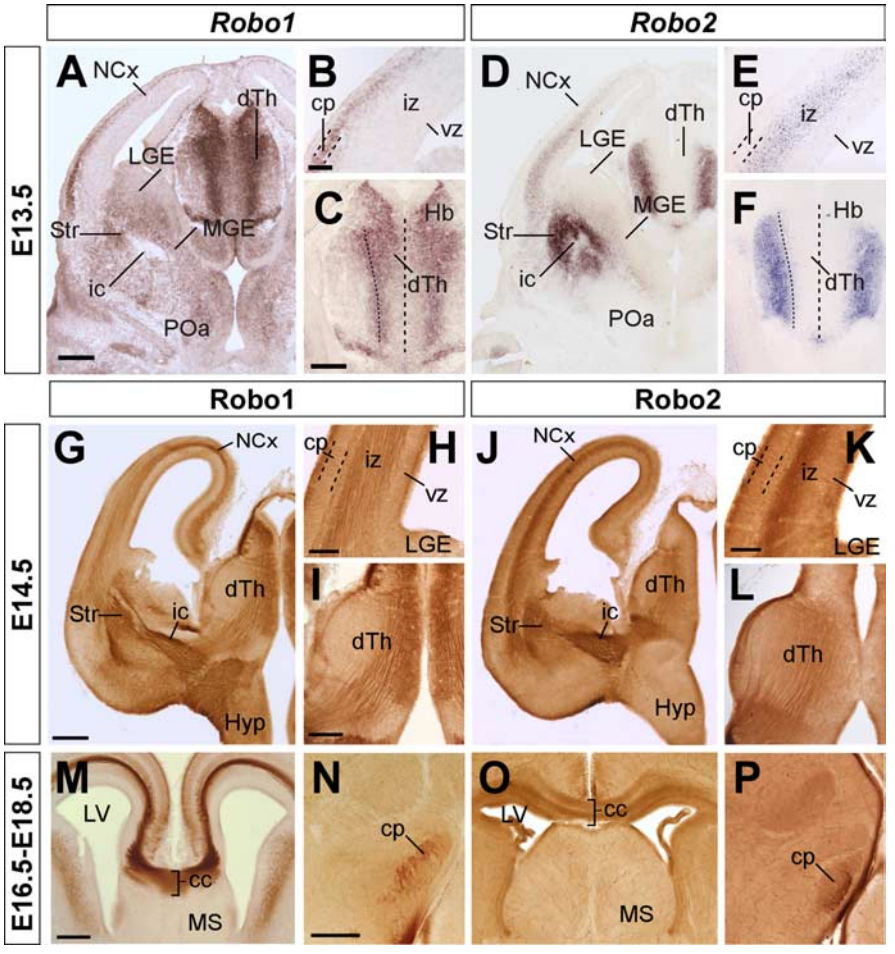

Figure 1. Expression of Robo1 and Robo2 receptors in the embryonic mouse forebrain. Serial coronal sections through mid-telencephalic/rostral diencephalic levels of an E13.5 embryo showing the expression of *Robo1* and *Robo2* mRNAs (***A–D***), and of E14.5, E16.5, and E18.5 embryos showing the expression of Robo1 (***G–I***, ***M***, ***N***) and Robo2 proteins (***J–L***, ***O***, ***P***). *Robo1* and *Robo2* mRNAs are expressed in the neocortex (NCx) and dorsal thalamus (dTh) in a partially complementary manner. *Robo1* is expressed in the cortical plate (cp) (***A***, ***B***), in a gradient decreasing from lateral to medial cortex, as well as in the dTh, in a gradient decreasing from the neuroepithelium to the mantle (***A***, ***C***). *Robo2* is expressed in the subplate and intermediate zone (iz) of the cortex (***D***, ***E***), and in the most superficial region of the dTh (***D***, ***F***). Coronal sections through E14.5, E16.5, and E18.5 brains showing Robo1 (***G–I***, ***M***, ***N***) and Robo2 (***J–L***, ***O***, ***P***) protein expression pattern are shown. Robo1 and Robo2 receptors are expressed in developing axons localized at the iz of the cortex (***G***, ***H***, ***J***, ***K***), dorsal thalamus (***I***, ***L***), and corpus callosum (cc) (***M***, ***O***), and in the cerebral peduncle (cp) (***N***). ic, Internal capsule; Hb, habenula; vz, ventricular zone; Str, striatum; LGE, lateral ganglionic eminence; MGE, medial ganglionic eminence; MS, medial septum; MPO, medial preoptic area; LV, lateral ventricle; Hyp, hypothalamus; VMH, ventromedial hypothalamic nucleus. Scale bars: ***A***, ***D***, ***G***, ***J***, 300 μm; ***B***, ***E***, ***H***, ***K***, ***M***, ***O***, 100 μm; ***C***, ***F***, ***I***, ***L***, ***K***, ***L***, ***N***, ***P***, 200 μm.

cortical plate primarily express *Robo1* (Fig. 1*B*). Conversely, dorsal thalamic neurons predominantly express *Robo1* as they first become postmitotic (Fig. 1*C*), but they mostly express *Robo2* once they start to differentiate into distinct nuclei of the dorsal thalamus (Fig. 1*F*).

Despite these apparent differences at the mRNA level, immunohistochemistry against Robo1 and Robo2 demonstrated that axons in both corticofugal and thalamocortical projections express both receptors (Fig. 1*G–L*). Moreover, both receptors are also expressed in corticospinal (Fig. 1*N*,*P*) (for simplicity, we use through the text the term "corticospinal" to refer to cortical layer 5 projections directed toward the mesencephalon, pons, and spinal cord) and callosal projections (Fig. 1*M*,*O*). In agreement with these results, analysis of Slit binding sites using Slit1 and Slit2 probes fused to AP tags revealed that callosal, thalamocortical, corticothalamic, and corticospinal axons contain receptors that bind both Slit1 and Slit2 (Fig. 2*A–D*) (data not shown). Slit–AP binding was also detected in the absence of either one of the Robo receptors, reinforcing the notion that Robo1 and Robo2 are mostly coexpressed in these projections (Fig. 2*E*,*F*) (data not shown). In contrast, Slit2–AP probes did not stain callosal, thalamocortical, corticothalamic, or corticospinal axons in tissue obtained from *Robo1;Robo2* double mutants (Fig. 2*H*) (data not shown), whereas Slit1–AP probes revealed only slight staining in some of these fibers tracts (Fig. 2*G*) (data not shown).

In summary, the temporal and spatial pattern of Robo1 and Robo2 expression in cortical and dorsal thalamic axons suggest that these receptors may play a role in the guidance of the major forebrain axonal tracts, probably mediating the function of Slit proteins in this process.

Slit2 repels neocortical and dorsal thalamic axons *in vitro*

The previous results strongly suggest that cortical and thalamic axons respond to Slit proteins through both Robo1 and Robo2 receptors. In agreement with this view, it has been previously shown that cortical axons are repelled by Slit2 *in vitro* (Shu and Richards, 2001) (supplemental Fig. 1, available at www.jneurosci.org as supplemental material). However, the effect of Slits on thalamic axons has not been tested. To examine the role of Slit proteins on thalamic axons, we cocultured E13.5 dTh explants with COS cells aggregates expressing *Slit2* in three-dimensional collagen gels (Fig. 3). After 4 d *in vitro*, axons extended radially from explants in control experiments (Fig. 3*A*,*D*) ($n = 19$). In contrast, axon length was significantly shorter on the side of explants facing COS cells aggregates expressing *Slit2* (Fig. 3*B*,*D*) ($n = 22$). Moreover, we observed many axons turning away from COS cells aggregates expressing *Slit2* (Fig. 3*B*, arrow). These results suggest that, as in the case of cortical axons, Slits proteins also repel the growth of dorsal thalamic axons.

Abnormal corticospinal and thalamocortical projections in *Robo2* but not *Robo1* mutants

The mostly complementary protein expression pattern of Robo1 and Robo2 in the developing forebrain axons suggests that these receptors may coordinate their activity in the guidance of cortical and thalamic projections. To directly address the role of individual Robo receptors in the guidance of these axonal tracts, we first examined the organization of these axons in mice carrying loss-of-function alleles of *Robo1* or *Robo2*. At E18.5, when most forebrain connections have been established, immunohistochemistry for the cell adhesion molecule L1 labels both corticothalamic and thalamocortical axons as they course through the internal capsule in the basal ganglia (Fig. 4*A*) (Jones et al., 2002; López-Bendito et al., 2002). The distribution of L1+ fibers in the telencephalon of

balt6/zns-neusci/zns-neusci/zns-orig/zns3079-07a | simmsl | S=3 | 3/6/07 | 10:42 | Art: 3203943 | Input-YY(v)

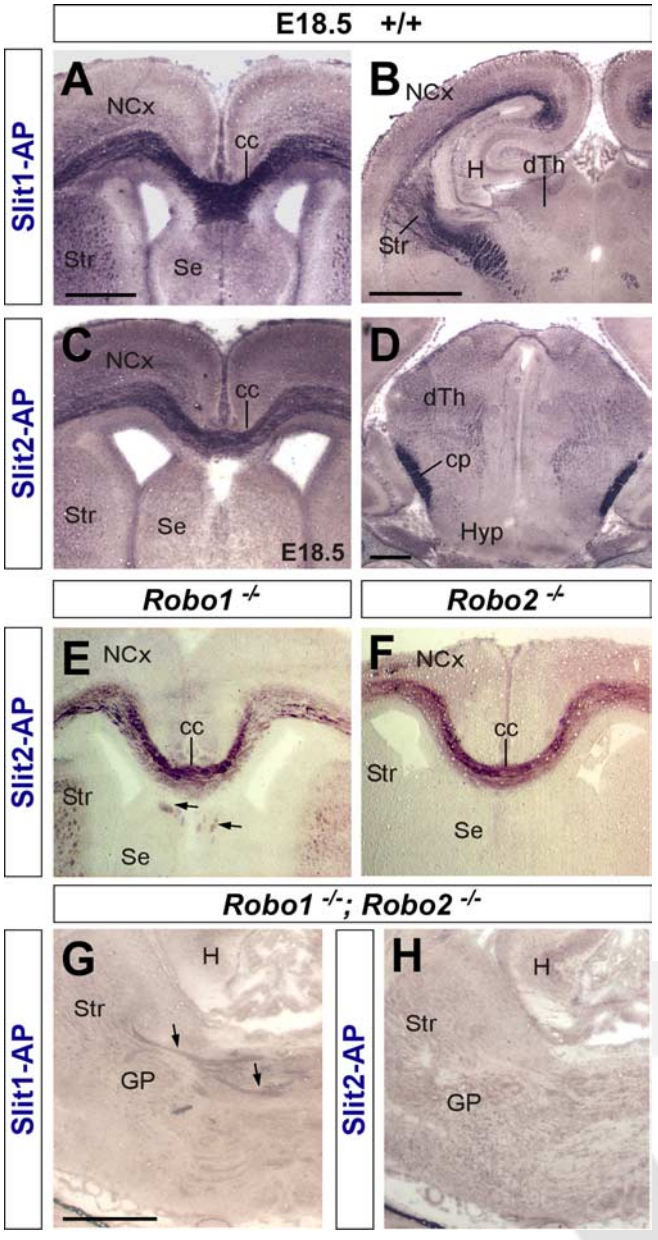

Figure 2. Coronal sections through the forebrain of E18.5 wild-type (***A–D***), *Robo1* (***E***), *Robo2* (***F***), and *Robo1;Robo2* double-mutant (***G***, ***H***) fetuses showing Slit1–AP binding (***A***, ***B***, ***G***) and Slit2–AP binding (***E***, ***F***, ***H***). ***A–D***, AP staining labels corticocortical axons at the corpus callosum (cc) (***A***, ***C***), corticospinal axons at the cerebral peduncle (cp) (***D***), and thalamocortical/corticothalamic projections (***B***). ***E***, ***F***, Slit2–AP staining identifies corticocortical callosal projections in *Robo1* (***E***) and *Robo2* (***F***) mutant brains. Some ectopic bundles are abnormally displaced at the corpus callosum (cc) of *Robo1 mutants* (***E***, arrows). ***G***, ***H***, Slit–AP binding assays do not generally stain any axonal tract in the forebrain of *Robo1;Robo2* double mutants. Only in a few cases, very weakly stained fibers could be observed after Slit1–AP binding (***G***, arrows). H, Hippocampus; Str, striatum; NCx, neocortex; SE, septum; dTh, dorsal thalamus; GP, globus pallidus; Hyp, hypothalamus; HC, hippocampal commissure. Scale bars: ***A***, ***C***, ***E***, ***F***, 500 μm; ***B***, ***G***, ***H***, 1 mm; ***D***, 200 μm.

Robo1 or *Robo2* single mutants was mostly indistinguishable from control mice ($n = 8$ for each genotype) (Fig. 4*A–C*). Moreover, labeling of axons with DiI crystals placed in the neocortex of E18.5 *Robo1* or *Robo2* single mutants did not reveal major differences in the distribution of corticofugal axons as they course through the internal capsule (Fig. 5*A–C*). In some *Robo2* mutants, however, a few corticofugal axons were found ventrally displaced, abnormally reaching the ventral midline at the level of the anterior commissure ($n = 4$ of 8 brains) (Fig. 5*C′*).

Immunohistochemistry for NPY, a transient marker of corticothalamic projections (Bagri et al., 2002), did not reveal major differences in the distribution of corticothalamic axons in either *Robo1* or *Robo2* single mutants ($n = 4$ for each genotype) (Fig. 4*D–F*). Similar results were obtained from the analysis of corticothalamic axons after DiI placements in the neocortex ($n = 8$ for each genotype) (Fig. 5*D*,*E*) (data not shown). Occasionally, some abnormal bundles of cortical fibers were found in the dorsal thalamus of *Robo2* mutants ($n = 4$ of 8 brains) (Fig. 5*F*), suggesting the existence of targeting defects in a subset of mice lacking Robo2 function.

Because the development of corticothalamic and thalamocortical axons is highly coordinated in time and space (for review, see López-Bendito and Molnár, 2003), we next analyzed thalamocortical projections in *Robo1* and *Robo2* single mutants. Analysis of thalamocortical projections using immunohistochemistry against calretinin, a marker of thalamic axons, revealed a normal distribution of thalamocortical axons in *Robo1* mutants compared with controls ($n = 4$) (Fig. 4*G*,*H*) (data not shown). In contrast, in *Robo2* mutants, some thalamocortical fibers were observed to fail reaching the telencephalon, and instead growing abnormally toward the ventral diencephalon, a region normally nonpermissive for thalamocortical axon outgrowth ($n = 4$) (Fig. 4*I*) (Braisted et al., 1999). DiI injections in the dorsal thalamus of control, *Robo1* and *Robo2* mutants confirmed that numerous thalamocortical axons failed to enter the telencephalon and instead invaded the hypothalamus in *Robo2* mutants (Fig. 5*I*), whereas no major defects were observed in the guidance of thalamocortical axons in *Robo1* mutants compared with wild-type control brains ($n = 4$) (Fig. 5*G*,*H*).

We next studied the organization of other corticofugal projections, such as those contributing to cerebral peduncle or the corpus callosum. Analysis of the cerebral peduncle at the level of the diencephalon demonstrated that corticospinal axons develop normally in the absence of Robo1 function compared with wild-type controls ($n = 4$) (Figs. 4*J*,*K*, 5*J*,*K*). In contrast, the cerebral peduncle appears to be ventrally displaced in all *Robo2* mutants examined ($n = 4$) (Figs. 4*L*, 5*L*). Moreover, DiI-labeled corticofugal axons were observed to abnormally defasciculate from the cerebral peduncle in some *Robo2* mutants ($n = 3$ of 4 brains) (data not shown).

Previous studies have shown that Slit2 is required for the guidance of corticocortical projections at the corpus callosum (Bagri et al., 2002; Shu et al., 2003). However, analysis of Slit2–AP binding assays revealed only minor defects in the development of the corpus callosum in *Robo1* mutant embryos, and no apparent abnormalities in *Robo2* mutant embryos compared with controls ($n = 3$) (Fig. 2*E*,*F*). Immunohistochemistry against NPY ($n = 4$) (Fig. 4*M–O*) or DiI tracing from the neocortex ($n = 4$) (Fig. 5*M–O*) reinforced this view, because both methods failed to reveal major defects in the development of callosal projections in *Robo1* or *Robo2* single mutants.

Corticofugal axon guidance is severely disrupted in *Robo1;Robo2* double mutants

The mild defects seen in the single mutants suggested two possibilities: (1) Robo receptors do not mediate the function of Slit proteins during the development of forebrain connections, or (2) Robo1 and Robo2 receptors are mostly coexpressed and function cooperatively in corticofugal and thalamocortical axons. In the latter case, each Robo receptor may functionally compensate for

balt6/zns-neusci/zns-neusci/zns-orig/zns3079-07a | simmsl | S=3 | 3/6/07 | 10:41 | Art: 3203943 | Input-YY(v)

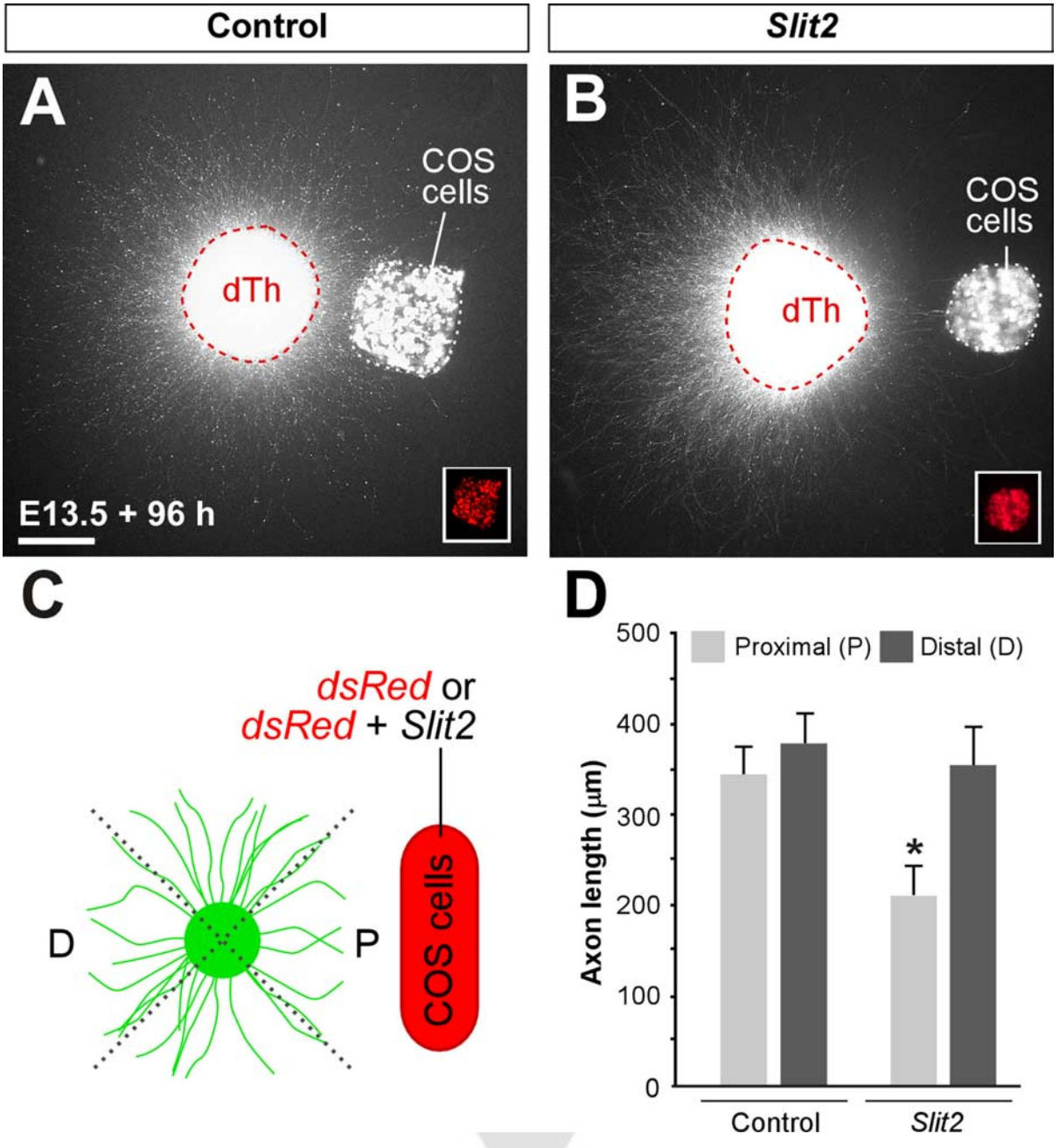

Figure 3. Dorsal thalamic explants from E13.5 GFP transgenic mice showing Slit2 repulsion to dorsal thalamic axons. ***A***, ***B***, Dorsal thalamic explants were cocultured in collagen for 4 d *in vitro* either with mock-transfected COS cells (***A***) or Slit2-transfected COS cells (***B***). ***C***, Scoring scheme used to test the effect of Slit2 on dorsal thalamus (dTh) axons in the experiments presented in ***A*** and ***B***. Explants were subdivided into four equal sectors. The two sectors used for quantification were designated as proximal (P) and distal (D) in relation to the COS cell aggregate. The length of the 13 longest axons in each sector was measured in every explant. ***D***, Quantification of the axonal growth of dTh explants cultured in collagen with mock-transfected COS cells ($n = 19$) or Slit2-transfected COS cells ($n = 22$) show a repulsive activity of Slit2. Mean length of axons was as follows: proximal, 345.8 ± 32.3 μm; distal, 374.9 ± 33.0 μm (average ± SEM) in controls; and proximal, 210.4 ± 29.4 μm; distal, 356.1 ± 43.5 μm (average ± SEM) in experimental cases. $p > 0.001$. Significant differences were observed among proximal sectors in the case of Slit2 compared with controls cases. Scale bar, 200 μm.

AQ: R

the loss of the other one, providing a rational explanation to the absence of guidance defects found in either *Robo1* or the relatively minor abnormalities present in *Robo2* single mutants. To test this hypothesis, we next examined the organization of cortical and thalamic projections in *Robo1;Robo2* double mutants.

In contrast to *Robo1* and *Robo2* single mutants, a simple cytoarchitectonical analysis of the telencephalon of *Robo1;Robo2* double mutants revealed the existence of large bundles of ectopic fibers crossing the ventral midline at E18.5 ($n = 5$) (Fig. 6*A–C*). This abnormal crossing of fiber tracts at the level of the anterior commissure was also observed on sections stained with antibodies against L1 ($n = 5$) (Fig. 6*D–F*). L1 and calbindin immunostaining on sagittal sections revealed even more clearly that, in addition to the anterior commissure, large bundles of axons aberrantly cross the midline in the basal telencephalon of *Robo1;Robo2* double mutants ($n = 3$) (Fig. 6*G–L*). Because of the presence of the ectopic commissural axons, the anterior commissure is always displaced dorsally in *Robo1;Robo2* double mutants (Fig. 6*K*,*L*).

F6

AQ: L

To determine the source of the ectopic commissural axons

balt6/zns-neusci/zns-neusci/zns-orig/zns3079-07a | simmsl | S=3 | 3/6/07 | 10:41 | Art: 3203943 | Input-YY(v)

found in the basal telencephalon of *Robo1; Robo2* double mutants, we next traced the trajectory of cortical axons by placing crystals of DiI in the developing neocortex. At E18.5, DiI injections in the parietal cortex of wild-type mice revealed a thick bundle of labeled axons coursing through the internal capsule as they progress toward the diencephalon ($n = 10$) (Fig. 7*A*,*B*). In contrast, DiI placements in the neocortex of *Robo1;Robo2* double mutants showed that most corticofugal axons were diverted toward the midline, which they abnormally crossed ($n = 8$) (Fig. 7*C*,*D*,*F*). Interestingly, many cortical axons appear to return toward the midline after crossing it (Fig. 7*D*,*F*), because only a few axons were found to grow away from the midline toward the contralateral cortex (data not shown). DiI injections in the neocortex, in particular its caudal part, labeled some axons that did not decussate in the ventral telencephalon but followed their normal route toward the diencephalon (Fig. 7*E*) (data not shown). The abnormal trajectory of corticofugal axons was observed in embryos as early as E14.5 ($n = 3$) (supplemental Fig. 2, available at www.jneurosci.org as supplemental material).

The massive number of axons that abnormally cross the ventral telencephalon in *Robo1;Robo2* double mutants suggests that both corticothalamic (layer 6) and cerebral peduncle (layer 5) projections are affected in the absence of Robo function. Accordingly, immunohistochemistry for NPY as well as DiI tracing experiments from the parietal cortex revealed that only a few cortical axons reach the dorsal thalamus in *Robo1;Robo2* double mutants ($n = 8$) (Fig. 8*A–D*,*G*,*H*). Moreover, these axons follow a more ventral trajectory than wild-type axons as they enter the diencephalon on their way to the dorsal thalamus (Fig. 8*A*,*B*,*G*,*H*).

Whereas some corticothalamic axons were consistently found in the absence of Robo1 and Robo2 function, DiI placements in the neocortex revealed that virtually no corticospinal axons reach the diencephalon through the cerebral peduncle in *Robo1;Robo2* double mutants ($n = 8$) (Fig. 8*E–H*). Thus, Robo1 and Robo2 appear essential for the normal development of layer 5 cortical projections.

Simultaneous loss of Robo1 and Robo2 perturbs corticocortical projections at the corpus callosum

We next analyzed whether the projections of corticocortical axons were also impaired in the absence of both receptors. At

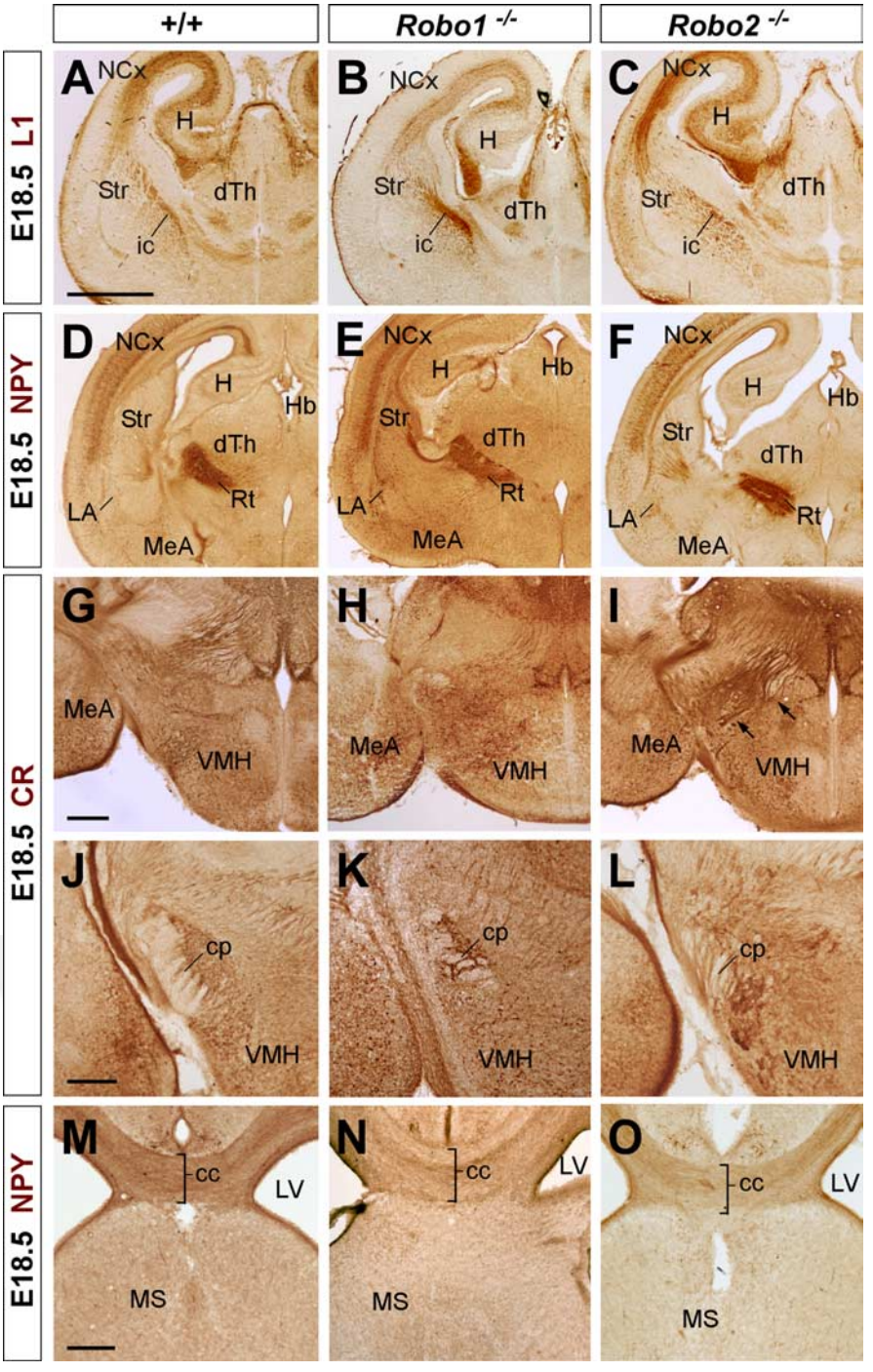

Figure 4. Abnormal axonal trajectories in the forebrain of Robo1 and Robo2 single-mutant mice. Coronal sections through the telencephalon of E18.5 embryos showing cell adhesion molecule L1 (L1) (***A–C***), NPY (***D–F***, ***M–O***), and calretinin (CR) (***G–I***) immunohistochemistry in wild-type (***A***, ***D***, ***G***, ***J***, ***M***), *Robo1* (***B***, ***E***, ***H***, ***K***, ***N***), and *Robo2* (***C***, ***F***, ***I***, ***L***, ***O***) mutant mice. ***A–C***, In wild-type embryos, L1+ axons are confined to the intermediate zone of the neocortex (NCx), striatum (Str), and dorsal thalamus (dTh). In *Robo1* and *Robo2* mutants, L1+ fascicles are observed at the NCx and Str in a similar pattern as in wild-type embryos. ***D–F***, Immunohistochemistry for NPY demonstrates that corticothalamic axons reach the diencephalon in wild-type (***D***), and *Robo1* (***E***) and *Robo2* mutant (***F***) brains. ***G–I***, Coronal sections at the level of the diencephalon showing the trajectory of thalamocortical axons by immunohistochemistry for calretinin (CR) in wild-type (***G***), and *Robo1* (***H***) and *Robo2* (***I***) mutant brains. At this level, CR+ thalamocortical axons normally turn rostrally to enter the telencephalon, thus leaving the plane of section as observed in wild-type (***G***) and *Robo1* mutants (***H***). In contrast, abnormal CR+ bundles were observed descending to the hypothalamus in *Robo2* mutants (***I***, arrows). ***J–L***, Abnormal development of the cerebral peduncle (cp) in *Robo2* mutant brains (***L***), as revealed by calretinin immunostaining. ***M–O***, Coronal sections at the level of the corpus callosum (cc) showing corticocortical fibers labeled by NPY immunohistochemistry in wild-type (***M***), and *Robo1* (***N***) and *Robo2* (***O***) mutant mice. ic, Internal capsule; H, hippocampus; Hb, habenula; Rt, reticular thalamic nucleus; VMH, ventromedial hypothalamic nucleus; MeA, medial amygdala; LA, lateral amygdala; MS, medial septum; LV, lateral ventricle. Scale bars: ***A–F***, 1 mm; ***G–L***, 100 μm; ***M–O***, 200 μm.

balt6/zns-neusci/zns-neusci/zns-orig/zns3079-07a | simmsl | S=3 | 3/6/07 | 10:41 | Art: 3203943 | Input-YY(v)

F9

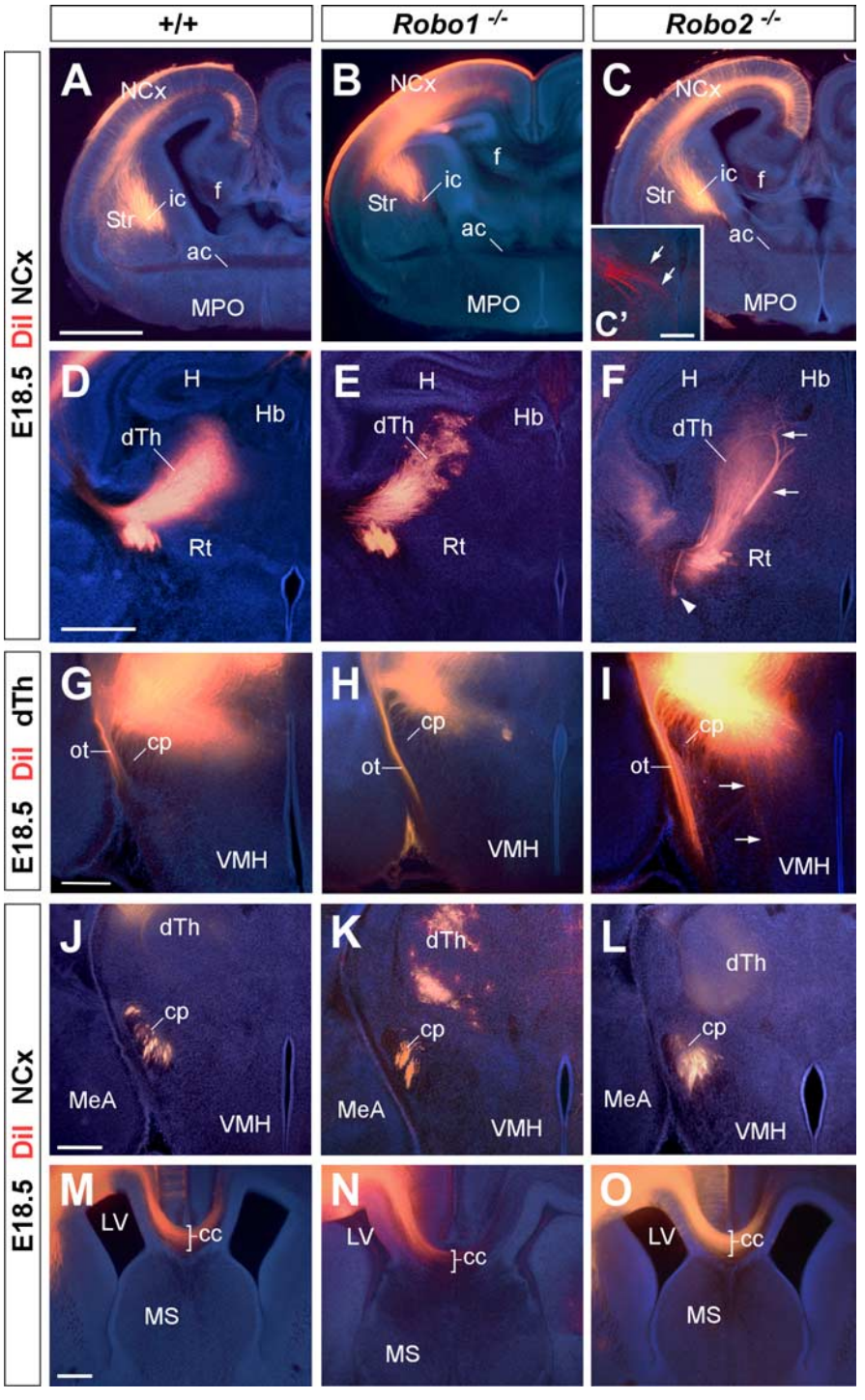

F10

Figure 5. Axon guidance defects in the forebrain of Robo2 single-mutant mice. Coronal sections through the telencephalon of E18.5 brains with DiI implanted in the neocortex (NCx) (***A–F***, ***J–O***) or in the dorsal thalamus (dTh) (***G–I***) of wild-type (***A***, ***D***, ***G***, ***J***, ***M***), and *Robo1* (***B***, ***E***, ***H***, ***K***, ***N***) and *Robo2* (***C***, ***F***, ***I***, ***L***, ***O***) mutant mice, showing computer-generated overlays of DiI-labeled axons and Hoechst counterstain. ***A–C′***, Coronal sections showing labeled DiI axons extending from the cortex into the internal capsule (ic) in wild-type (***A***), and *Robo1* (***B***) and *Robo2* (***C***, ***C′***) mutant mice. ***D–F***, Abnormal defasciculation (arrowhead) and targeting (arrows) of corticothalamic axons at the dorsal thalamus of *Robo2* mutant mice (***F***). In *Robo1* mutant mice, labeled axons extend from the cortex into the dorsal thalamus normally. ***G–I***, Coronal sections through the caudal diencephalon showing dorsal thalamic fibers abnormally entering the hypothalamus in *Robo2* mutant mice (***I***). No guidance defects were observed in the thalamocortical axons in *Robo1* mutant mice (***H***) compared with wild type (***G***). ***J–L***, Coronal sections showing corticospinal labeled axons at the cerebral peduncle (cp) of wild-type (***J***), and *Robo1* (***K***) and *Robo2* (***L***) mutant mice. Note the abnormal ventral position of the cerebral peduncle and the defasciculation of axons in *Robo2* mutant mice. ***M–O***, Rostral coronal sections showing corticocortical axons at the corpus callosum (cc) of wild-type (***M***), and *Robo1* (***N***) and *Robo2* (***O***) mutant mice. No guidance defects were observed in either of the *Robo* single mutants. ac, Anterior commissure; Str, striatum; f, fimbria; MPO, medial preoptic area; H, hippocampus; Rt, reticular thalamic nucleus; Hb, habenula; VMH, ventromedial hypothalamic nucleus; MeA, medial amygdala nucleus; LA, lateral amygdala; MS, medial septum; ot, optic tract; LV, lateral ventricle. Scale bars: ***A–C***, 1 mm; ***C′***, 200 μm; ***D–F***, 500 μm; ***G–O***, 300 μm.

AQ: S

E18.5, Nissl staining revealed that the size of the corpus callosum was reduced in *Robo1;Robo2* double mutants compared with wild-type mice ($n = 5$) (Fig. 9*A*,*B*). In addition, two large ectopic bundles of fibers were also found on either side of the corpus callosum of *Robo1;Robo2* double mutants, which resemble Probst bundles (Fig. 9*B*). These ectopic bundles were also observed when sections were stained for NPY ($n = 3$) (Fig. 9*D*). Moreover, DiI tracing experiments demonstrated that the ectopic axons were corticocortical axons that abnormally defasciculated from the corpus callosum and coursed ventrally into the septum ($n = 4$) (Fig. 9*E–H*). This defect was consistently observed after DiI placements in different cortical regions (data not shown).

Prominent thalamocortical axon guidance defects in *Robo1;Robo2* double mutants

We next investigated the consequences of the simultaneous loss of Robo1 and Robo2 receptors in the guidance of thalamocortical axons. At E18.5, immunohistochemistry against calretinin, which labels thalamocortical projections originating from medial thalamic nuclei, revealed that numerous thalamic axons abnormally invade the hypothalamus, failing to turn rostrally into the telencephalon ($n = 3$) (Fig. 10*A–C*,*M*,*N*). In agreement with this observation, DiI injections into the dorsal thalamus of E18.5 *Robo1;Robo2* double mutants showed that, compared with control mice, the vast majority of thalamocortical projections fail to enter the telencephalon and instead invade the hypothalamus ($n = 3$) (Fig. 10*G–I*,*M*,*N*), a phenotype that was observed already in E14.5 embryos ($n = 3$) (supplemental Fig. 2, available at www.jneurosci.org as supplemental material).

DiI injections in the dorsal thalamus revealed that only some thalamic axons enter the telencephalon in *Robo1;Robo2* double mutants. Once in the telencephalon, very few thalamocortical axons were found to grow through the internal capsule into the cerebral cortex ($n = 5$) (Fig. 10*J–L*,*M*,*N*). Instead, many of the thalamocortical fibers that succeeded in entering the telencephalon were abnormally diverted toward the midline, which they cross (Fig. 10*D–F*,*M*,*N*) (data not shown). In summary, thalamocortical projections are severely disrupted in the absence of Robo1 and Robo2 function, with many axons aberrantly projecting toward the hypothalamus or the telencephalic ventral midline.

balt6/zns-neusci/zns-neusci/zns-orig/zns3079-07a | simmsl | S=3 | 3/6/07 | 10:41 | Art: 3203943 | Input-YY(v)

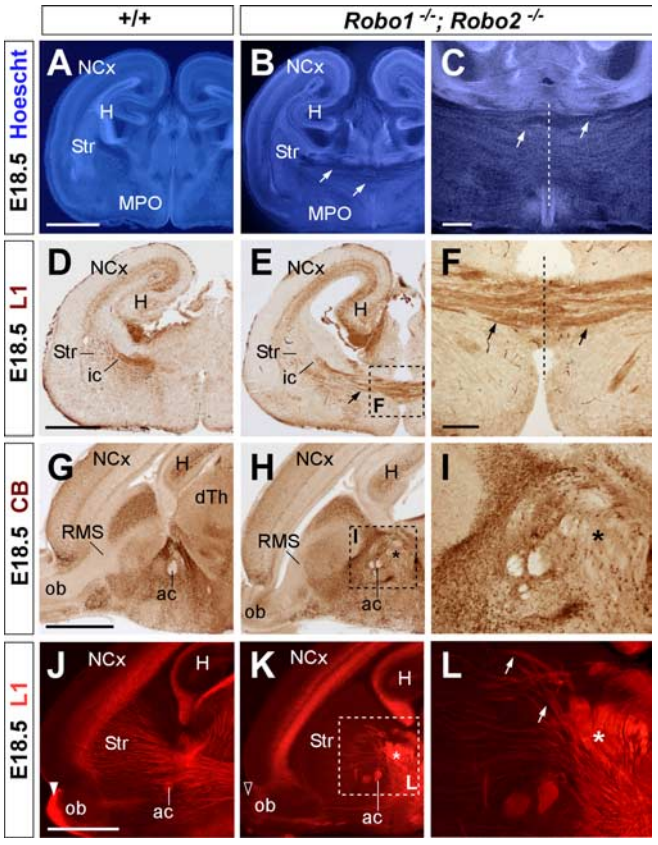

Figure 6. Abnormal axonal trajectories in the forebrain of *Robo1;Robo2* double-mutant mice. Coronal (***A–F***) and sagittal (***G–L***) sections through the telencephalon of E18.5 embryos showing Hoechst staining (***A–C***), cell adhesion molecule L1 (***D–F***, ***J–L***), and calbindin (***G–I***) immunohistochemistry in wild-type (***A***, ***D***, ***G***, ***J***) and *Robo1;Robo2* (***B***, ***C***, ***E***, ***F***, ***H***, ***I***, ***K***, ***L***) mutant mice. ***A–C***, Hoechst staining shows ectopic axonal bundles crossing the midline at the level of the medial preoptic region (MPO) (***B***, ***C***, arrows). The anterior commissure (ac) is severely displaced dorsally. ***D–F***, Immunostaining for L1 confirm that abnormal bundles of fibers cross the midline in *Robo1;Robo2* mutants (***E***, ***F***, arrows). ***G–I***, Immunohistochemistry for calbindin delineates the abnormal crossing of the midline by unstained fibers (***H***, ***I***). ***J–L***, Ectopic bundles of axons crossing the midline are very evident in sagittal sections. Very few thalamic L1+ axons extend through the striatum in *Robo1;Robo2* mutants because they accumulate in the midline (asterisk). The midline is indicated by a dotted line in ***C*** and ***F***. NCx, Neocortex; ic, internal capsule; ob, olfactory bulb, RMS, rostral migratory steam; Str, striatum; H, hippocampus. Scale bars: ***A***, ***B***, ***D***, ***E***, ***G***, ***H***, ***J***, ***K***, 1 mm; ***C***, 300 μm; ***F***, ***I***, ***L***, 200 μm.

Discussion

The functioning of the cerebral cortex relies on several stereotypical long-distance projections, such as the corticofugal, callosal, and thalamocortical connections. Several studies have examined the early development of these projections and have identified pioneering axonal populations as well as potential intermediate targets and choice points for these axons (McConnell et al., 1989; De Carlos and O'Leary, 1992; Métin and Godement, 1996; Molnár et al., 1998; Braisted et al., 1999; Tuttle et al., 1999; Auladell et al., 2000; López-Bendito et al., 2006). In addition, multiple molecules that participate in the guidance of these connections have been identified, providing a comprehensive frame in which to understand their development (Serafini et al., 1996; Métin et al., 1997; Richards et al., 1997; Braisted et al., 2000; Leighton et al., 2001; Bagri et al., 2002; López-Bendito et al., 2006). Thus, Slits play a fundamental role in the development of corticocortical callosal projections, layer 5 corticofugal projections toward the mesencephalon, pons, and spinal cord, and layer 6 corticothalamic projections (Bagri et al., 2002; Shu et al., 2003). Moreover, the development of the reciprocal thalamocortical projections also depends on Slit function (Bagri et al., 2002). Here, we demonstrate that the function of Slits in the guidance of these connections is mostly mediated by the coordinated activity of Robo1 and Robo2 receptors.

Robo1 and Robo2 have mostly redundant functions in forebrain axon guidance

Our previous analysis of *Slit1* and *Slit2* mutants led us to suggest that Slit proteins contribute in at least three different ways to the development of the mammalian forebrain: (1) the maintenance of the dorsoventral position of longitudinal axonal tracts by preventing axons from entering into ventral regions; (2) the prevention of axonal extension toward and across the midline; and (3) the channeling of axons into particular regions, such as commissures (Bagri et al., 2002). Slit1 and Slit2, which are expressed in partially overlapping patterns in the forebrain, cooperate to fulfill these functions: Slit2 is mostly responsible of preventing ventral invasion and axon channeling (1 and 3), whereas both Slit1 and Slit2 contribute to prevent midline crossing of ipsilateral tracts (2) (Fig. 11). F11

The finding that Robo1 and Robo2 proteins are expressed in developing forebrain axons at the time when these connections are formed, led us to hypothesize that these receptors may play an important role in their guidance. However, analysis of mouse mutants for *Robo1* or *Robo2* revealed very few guidance errors in the absence of either one of these receptors. In the case of *Robo2* mutants, our analysis revealed only relatively moderate defects in the dorsoventral position of corticofugal, corticothalamic, and thalamocortical tracts, which enter ventral regions that they normally avoid (Fig. 11). In the case of *Robo1* mutants, we could detect only very minor defects in the development of some corticocortical callosal connections (Fig. 2*E*). In contrast to our findings, a recent analysis of a different mutant allele of *Robo1* showed a more severe phenotype, demonstrating that the function of this receptor is essential for the development of callosal projections, the absence of which cannot be compensated by the function of Robo2 (Andrews et al., 2006). We do not know the AQ: M source of the discrepancy; however, it is possible that, as previously observed with other genes (Zheng et al., 2003), differences in the genetic background of the two mutant strains could explain the different penetrance of the *Robo1* mutation. In addition, our *Robo1* allele is likely to be a severe hypomorph rather than a complete null (Long et al., 2004); this would be consistent with the observation of weak Slit1–AP binding in *Robo1;Robo2* double mutants (Fig. 2*G*). In any case, our *Robo1* allele only appears to behave as a hypomorph in the callosal projection [compared with the *Robo1* allele described by Andrews et al. (2006)], because the remaining defects observed in *Robo1;Robo2* double mice phenocopy those found in *Slit1;Slit2* double mutants.

The absence of severe axon guidance defects in *Robo1* and *Robo2* single mutants suggests that both receptors cooperate in the guidance of most forebrain projections. However, as described above for the callosal projections in *Robo1* mutants (this study; Andrews et al., 2006), there are defects in *Robo2* mutants that cannot be compensated by Robo1 function, such as the ventrally projecting axons found in corticofugal and thalamocortical tracts. This suggests that that Robo1 and Robo2 functions may not be completely redundant. Interestingly, cortical and thalamic projections also overshoot ventrally in *Slit2*, but not in *Slit1* mutants, which led to the proposal that the range of Slit2 function includes regions more distant from the midline than Slit1 (Fig.

balt6/zns-neusci/zns-neusci/zns-orig/zns3079-07a | simmsl | S=3 | 3/6/07 | 10:41 | Art: 3203943 | Input-YY(v)

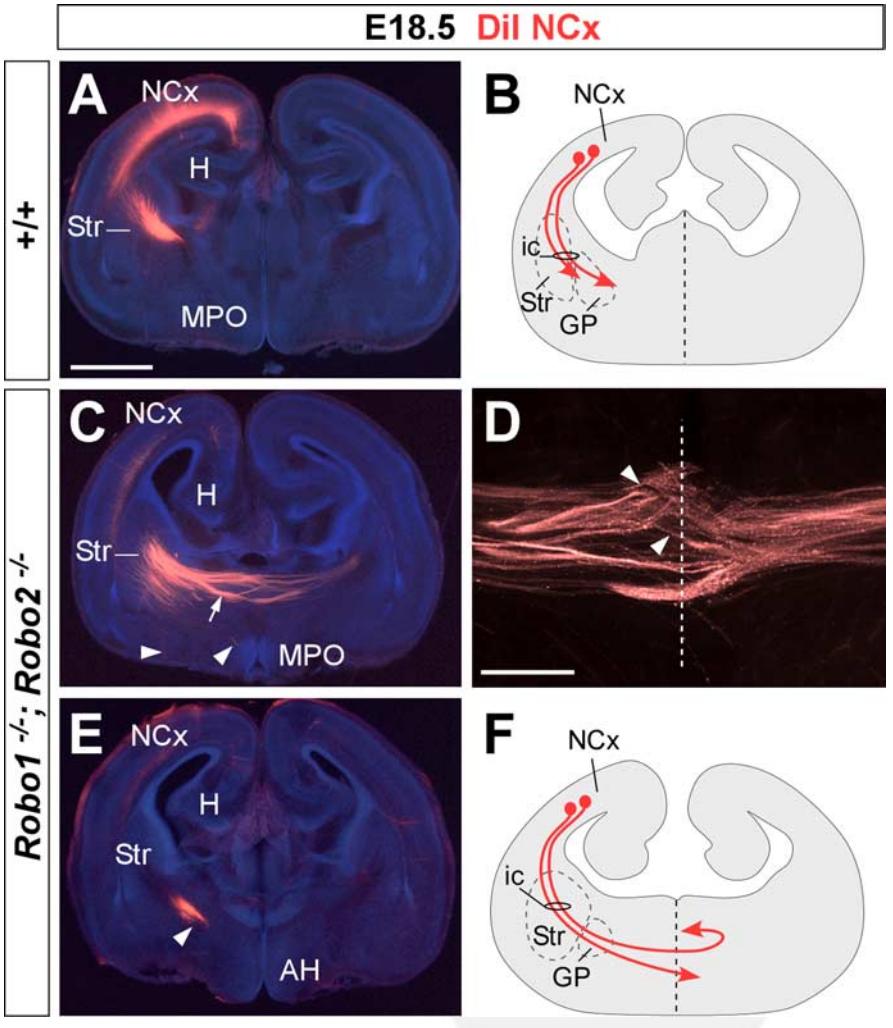

Figure 7. Corticofugal axons abnormally reach the telencephalic midline in *Robo1;Robo2* double-mutant mice. Coronal sections through the telencephalon of E18.5 brains with DiI implanted in the neocortex (NCx), showing computer-generated overlays of DiI-labeled corticofugal axons and Hoechst counterstaining from wild-type (***A***) and *Robo1;Robo2* mutants (***C–E***). The midline is indicated with a dotted line in ***D***. The schemas summarize the results obtained in control (***B***) and *Robo1;Robo2* mutants (***F***). ***A***, ***B***, In wild-type mice, labeled axons extend from the cortex into the striatum (Str). ***C–F***, In *Robo1;Robo2* mutants, labeled axons from the internal capsule (ic) abnormally approach the midline and cross it (***C***, arrow). A few axons that reach the midline course ventrally (arrowheads). Most of the axons that crossed the midline at more anterior levels were found in the contralateral side, where they either travel to the base of the telencephalon or extend toward the contralateral cortex (***C***, ***D***). MPO, Medial preoptic area; H, hippocampus, AH, anterior hypothalamus. Scale bars: ***A***, ***C***, ***E***, 1 mm; ***D***, 300 μm.

11) (Bagri et al., 2002). Why do axons overshoot ventrally in *Robo2* mutants? One possibility is that some cortical and thalamic neurons do not express significant levels of Robo1 receptors. This is unlikely, however, because in the absence of both receptors axons abnormally cross the midline, and *Robo2* mutants do not have obvious midline crossing defects. Alternatively, Slit2 binding to Robo2 may be more effective than it is to Robo1, which therefore may not be able to mediate the repulsion required to maintain growing axons at their normal dorsoventral position (Fig. 11). Consistent with this possibility, full-length Slit2 or its proteolytic N-terminal fragment bind more effectively to Robo2 than to Robo1 *in vitro* (Nguyen Ba-Charvet et al., 2001). Thus, it is conceivable that the interaction between Slit2 and Robo2 constitutes the primary signaling system involved in maintaining the dorsoventral position of corticofugal and thalamocortical projections.

Similar forebrain guidance defects in *Robo1;Robo2* and *Slit1;Slit2* double mutants

The lack of prominent forebrain axon guidance defects in *Robo1* and *Robo2* mutants suggests that both receptors are indeed expressed by the same neurons and thereby may primarily compensate each other's function in the absence of one of the receptors. This compensation does not appear to be at the level of gene expression or protein localization, because Robo1 protein or mRNA levels do not change in the forebrain of *Robo2* mutant mice, and, conversely, Robo2 protein or mRNA levels do not vary in *Robo1* mutants (supplemental Figs. 3, 4, available at www.jneurosci.org as supplemental material). Instead, it seems most likely that cortical and thalamic neurons normally contain functional levels of both receptors in growing axons. This hypothesis is agreement with the analysis of *Robo1;Robo2* double mutants, which mostly recapitulate the phenotypes observed in *Slit1;Slit2* double mutants (Bagri et al., 2002) (Fig. 11).

In *Slit1;Slit2* double mutants, most corticofugal and corticothalamic axons fail to reach the diencephalon, because they massively cross the midline in the ventral telencephalon (Bagri et al., 2002). Thalamocortical axons also make prominent guidance errors in *Slit1;Slit2* double mutants; many run into the hypothalamic region, and the few that enter the telencephalon also turn aberrantly toward the midline. Thus, in the simultaneous absence of Slit1 and Slit2 or Robo1 and Robo2, cortical and thalamic ipsilateral projections fail to maintain their ipsilateral condition and instead abnormally invade the midline. Because these prominent defects are not present in either *Robo1* or *Robo2* single mutants (this study; Andrews et al., 2006), it seems clear that Slit1 and Slit2 prevent midline crossing of ipsilateral projections in the mammalian forebrain through both Robo1 and Robo2 receptors.

In the spinal cord, commissural axons upregulate Robo1 and Robo2 once they have crossed the midline, thereby contributing to their navigation beyond the floor plate (Long et al., 2004). In contrast, the only population of commissural axons examined in this study, the corticocortical callosal axons, is sensitive to Slit proteins before midline crossing. In this region, two glial populations adjacent to the midline, the glial wedge and the indusium griseum, express *Slit2* and form a narrow pathway through which callosal axons extend (Shu et al., 2003). It has been recently suggested that Robo1 might be the unique mediator of Slit2 function in the formation of the corpus callosum (Andrews et al., 2006). Our results, however, strongly suggest that Robo2 also contributes to the formation of this commissure, because we observed very prominent defects in *Robo1;Robo2* double mutants but no abnormalities in either *Robo1* or *Robo2* single mutants. Even as-

balt6/zns-neusci/zns-neusci/zns-orig/zns3079-07a | simmsl | S=3 | 3/6/07 | 10:41 | Art: 3203943 | Input-YY(v)

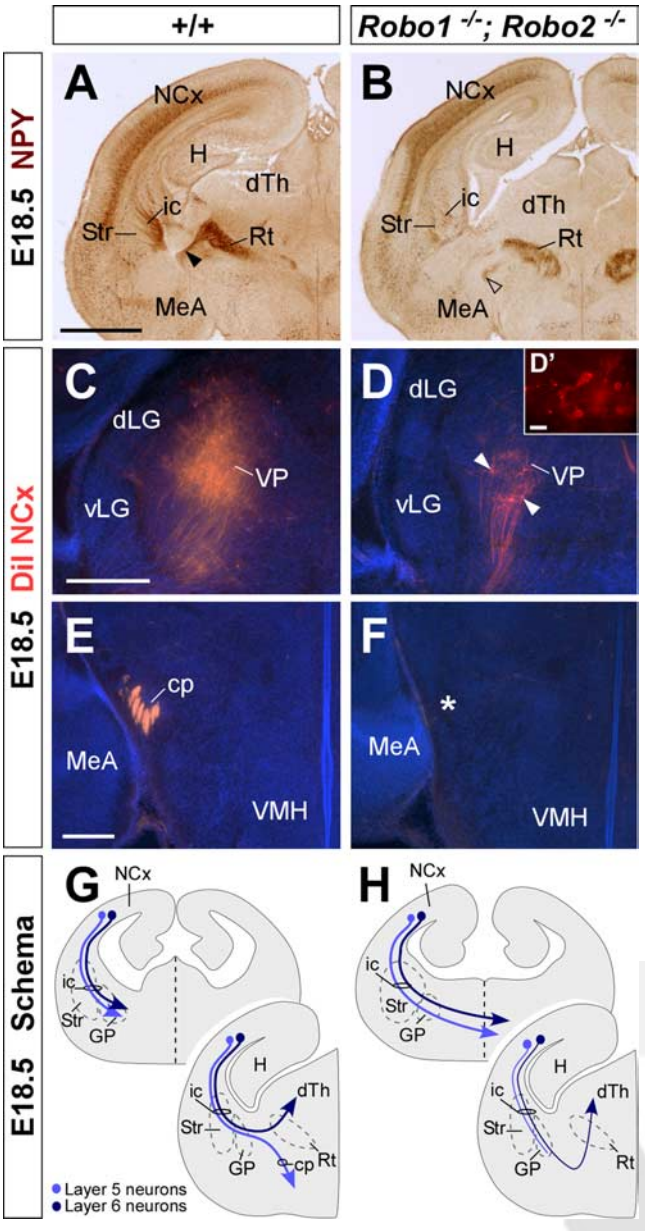

Figure 8. Corticothalamic and corticospinal projections are severely defective in *Robo1;Robo2* double-mutant mice. ***A***, ***B***, Coronal sections through the telencephalon of E18.5 brains showing NPY immunohistochemistry in wild-type (***A***) and *Robo1;Robo2* (***B***) mutant mice. NPY immunohistochemistry demonstrates that some cortical axons reach the dorsal thalamus (dTh) in *Robo1;Robo2* mutants, although through an abnormally ventral path (open arrowhead). ***C***, ***D***, Coronal sections through the dTh of E18.5 embryos with DiI implanted in the neocortex (NCx), showing computer-generated overlays of DiI retrogradely labeled cells and Hoechst counterstain from wild-type (***C***) and *Robo1;Robo2* mutants (***D***). The number of retrogradely labeled cells found in the dTh is greatly reduced in *Robo1;Robo2* mutants (***D***, arrowheads). ***E***, ***F***, The cerebral peduncle (cp) is absent in *Robo1;Robo2* mutants (***F***), as revealed by the lack of DiI-labeled corticospinal fibers in the structure. The majority of these fibers cross abnormally the midline at more rostral levels. ***G***, ***H***, The schemas summarize the pathway followed by corticothalamic (layer 6; dark blue) and corticospinal (layer 5; light blue) axons in wild-type (***G***), and *Robo1;Robo2* (***H***) mutant mice. Str, Striatum; Rt, reticular thalamic nucleus; VMH, ventromedial hypothalamic nucleus; MeA, medial amygdala; VP, ventroposterior nucleus; dLG, dorsal lateral geniculate nucleus, vLG, ventrolateral geniculate nucleus; ic, internal capsule; GP, globus pallidus; H, hippocampus. Scale bars: ***A***, ***B***, 1 mm; ***C***, ***D***, 300 μm; ***D'***, 10 μm; ***E***, ***F***, 200 μm.

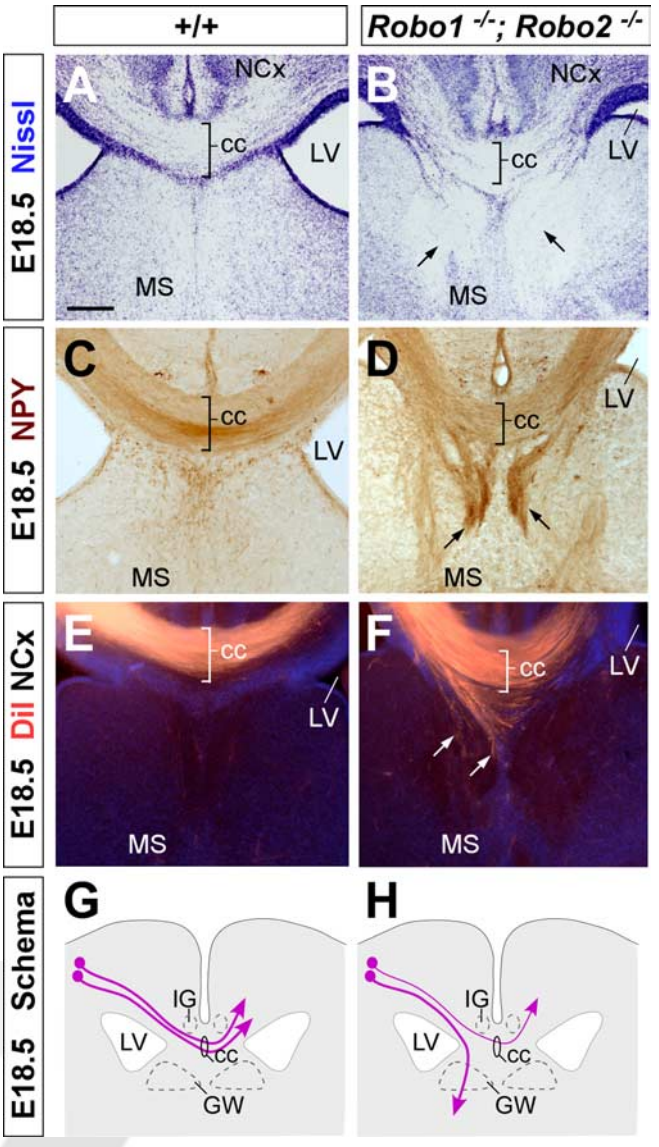

Figure 9. Abnormal development of the corpus callosum in *Robo1;Robo2* double-mutant mice. Coronal sections through the telencephalon of E18.5 fetuses showing Nissl stain (***A***, ***B***) and NPY (***C***, ***D***) immunohistochemistry in wild-type (***A***, ***C***) and *Robo1;Robo2* double-mutant mice (***B***, ***D***) mutant mice. ***A–D***, Nissl staining and NPY immunohistochemistry demonstrates that *Robo1;Robo2* double-mutant mice have a small corpus callosum (cc) and that large ectopic bundles of axons form on either side of it (***B***, ***D***, arrows). ***E***, ***F***, Coronal sections through the telencephalon of E18.5 fetuses with DiI implanted in the neocortex (NCx), showing DiI-labeled corticocortical axons extending through the corpus callosum in wild-type (***E***) and *Robo1;Robo2* double-mutant (***F***) mice. Note that many axons are abnormally directed ventrally before they reach the midline (***F***, arrows). ***G***, ***H***, The schemas summarize the pathways followed by corticocortical axons through the corpus callosum in wild-type (***G***) and *Robo1;Robo2* double-mutant (***H***) mice. MS, Medial septum; LV, lateral ventricle; GW, glial wedge; IG, indusium griseum. Scale bars: ***A–F***, 200 μm.

suming that the *Robo1* allele analyzed here is only a severe hypomorph, our genetic analysis strongly suggests that Robo2 signaling contributes along with Robo1 in the formation of the corpus callosum.

Interaction of Slit/Robo signaling with other molecules

It has been previously shown that molecules such as cell surface heparan sulfates may modulate the interaction of Slits and Robo receptors. Thus, biochemical experiments have shown that Slits bind the heparan sulfate proteoglycan glypican-1 (Liang et al., 1999; Ronca et al., 2001). Heparan sulfate enhances the affinity of Slit2 for Robo1 receptors *in vitro*, and removal of cell surface heparan sulfate by heparinase III treatment or addition of saturating amounts of heparan sulfate abolishes the repulsive activity of Slit2 toward olfactory bulb axons in explant cultures (Hu,

balt6/zns-neusci/zns-neusci/zns-orig/zns3079-07a | simmsl | S=3 | 3/6/07 | 10:41 | Art: 3203943 | Input-YY(v)

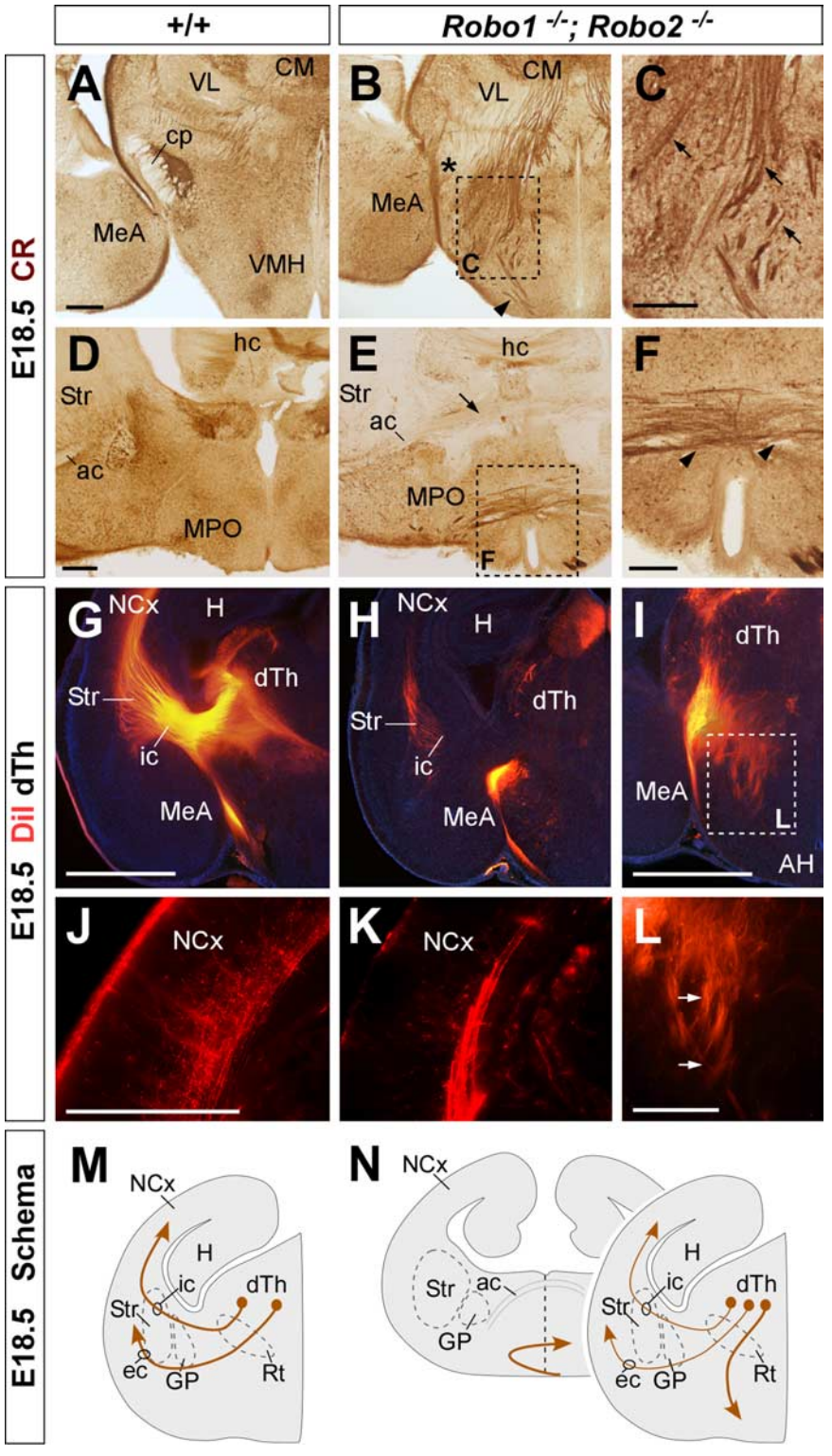

Figure 10. Thalamocortical axons follow abnormal paths in *Robo1;Robo2* double-mutant mice. ***A–F***, Coronal sections through the diencephalon of E18.5 fetuses showing calretinin immunohistochemistry in wild-type (***A***, ***D***) and *Robo1;Robo2* double-mutant mice (***B***, ***C***, ***E***, ***F***). Note the abnormal invasion of thalamocortical fibers into the hypothalamus (***C***, arrows). At more rostral levels, thalamocortical axons cross the ventral midline (***F***, arrowheads) below the additional abnormal cross of corticofugal fibers (***E***, arrow). ***G–I***, ***L***, Coronal sections through the diencephalon of E18.5 embryos with DiI implanted in the dorsal thalamus (dTh), showing DiI axons abnormally entering the hypothalamus in *Robo1;Robo2* double-mutant mice (***H***, ***I***). ***J***, ***K***, Very few thalamic axons reach the cortex in *Robo1;Robo2* double-mutant mice. ***M***, ***N***, The schemas summarize the pathways followed by thalamocortical axons in wild-type (***M***) and *Robo1;Robo2* double-mutant mice (***N***). Str, Striatum; VMH, ventromedial hypothalamic nucleus; MeA, medial amygdala; cp, cerebral peduncle; ac, anterior commissure; ic, internal capsule; ec, external capsule; GP, globus pallidus; Rt, reticular thalamic nucleus; MPO, medial preoptic area; hc, hippocampal commissure; H, hippocampus, AH, anterior hypothalamus. Scale bars: ***A***, ***B***, ***D***, ***E***, 300 μm; ***C***, ***F***, 200 μm; ***G–I***, 1 mm; ***J–L***, 200 μm.

2001). Moreover, nervous system-specific conditional mutants for EXT1, a glycosyltransferase enzyme required for the synthesis of heparan sulfate, display guidance defects at the optic chiasm that are similar to those found in *Slit1;Slit2* double mutants (Plump et al., 2002; Inatani et al., 2003). Furthermore, reduction of one *Ext1* allele in *Slit2*$^{-/-}$ mice, which otherwise have a relatively normal optic chiasm, cause profound retinal axon misguidance similar to those found in conditional *Ext1* mutants and *Slit1;Slit2* double mutants. Similarly, zebrafish mutants for both *ext2* (*dackel*, *dak*) and *extl3* (*boxer*, *box*), two additional glycosyltransferases implicated in heparan sulfate biosynthesis, show retinal axon guidance defects that phenocopy *robo2* mutants (Hutson and Chien, 2002; Lee et al., 2004). Together, these results suggest that heparan sulfate plays a physiologically essential role in Slit/Robo-mediated retinal axon guidance at the optic chiasm.

Although heparan sulfate may function in the extracellular environment, some evidence suggests that it may also or instead function on the surface of Robo-expressing, Slit responding cells, where it may contribute to concentrate Slit protein and promote its binding to Robo receptors. In the telencephalon, thalamic neurons express the heparan sulfate proteoglycan N-syndecan (Kinnunen et al., 1999), and both corticofugal and thalamocortical axons are labeled with antibodies against heparan sulfate (J. A. Sánchez and O. Marín, unpublished observations). Thus, it is conceivable that heparan sulfate may also contribute along with Slit/Robo signaling to the guidance of these major forebrain projections.

Concluding remarks

The present results, along with our previous work on the analysis of *Slit* mutants (Bagri et al., 2002), demonstrate that Slit/Robo interactions play a crucial role in the guidance of some of the most prominent axonal tracts in the mammalian forebrain. Through a mechanism that involves the repulsion of growing axons (Brose et al., 1999; Kidd et al., 1999; Li et al., 1999), Slits intervene in multiple aspects in the development of major connections in the mammalian forebrain. These functions appear to be mediated mostly or exclusively by Robo1 and Robo2, because the forebrain phenotype of *Robo1;Robo2* double mutants looks highly similar, and possibly identical to the *Slit1;Slit2* double-mutant phenotype. Furthermore, Robo1 and Robo2 have mostly redundant roles in

balt6/zns-neusci/zns-neusci/zns-orig/zns3079-07a | simmsl | S=3 | 3/6/07 | 10:41 | Art: 3203943 | Input-YY(v)

this process. Future studies will aim to reveal how Robo1 and Robo2 receptors are specifically regulated in distinct forebrain axonal tracts and how these receptors may interact with other guidance cues to control their final targeting.

References

Andrews W, Liapi A, Plachez C, Camurri L, Zhang J, Mori S, Murakami F, Parnavelas JG, Sundaresan V, Richards LJ (2006) Robo1 regulates the development of major axon tracts and interneuron migration in the forebrain. Development 133:2243–2252.

Auladell C, Pérez-Sust P, Supèr H, Soriano E (2000) The early development of thalamocortical and corticothalamic projections in the mouse. Anat Embryol 201:169–179.

Bagri A, Marín O, Plump AS, Mak J, Pleasure SJ, Rubenstein JL, Tessier-Lavigne M (2002) Slit proteins prevent midline crossing and determine the dorsoventral position of major axonal pathways in the mammalian forebrain. Neuron 33:233–248.

Braisted JE, Tuttle R, O'Leary DD (1999) Thalamocortical axons are influenced by chemorepellent and chemoattractant activities localized to decision points along their path. Dev Biol 208:430–440.

Braisted JE, Catalano SM, Stimac R, Kennedy TE, Tessier-Lavigne M, Shatz CJ, O'Leary DD (2000) Netrin-1 promotes thalamic axon growth and is required for proper development of the thalamocortical projection. J Neurosci 20:5792–5801.

Brose K, Bland KS, Wang KH, Arnott D, Henzel W, Goodman CS, Tessier-Lavigne M, Kidd T (1999) Slit proteins bind Robo receptors and have an evolutionarily conserved role in repulsive axon guidance. Cell 96:795–806.

De Carlos JA, O'Leary DD (1992) Growth and targeting of subplate axons and establishment of major cortical pathways. J Neurosci 12:1194–1211.

Dufour A, Seibt J, Passante L, Depaepe V, Ciossek T, Frisen J, Kullander K, Flanagan JG, Polleux F, Vanderhaeghen P (2003) Area specificity and topography of thalamocortical projections are controlled by ephrin/Eph genes. Neuron 39:453–465.

Grieshammer U, Le M, Plump AS, Wang F, Tessier-Lavigne M, Martin GR (2004) SLIT2-mediated ROBO2 signaling restricts kidney induction to a single site. Dev Cell 6:709–717.

Hao JC, Yu TW, Fujisawa K, Culotti JG, Gengyo-Ando K, Mitani S, Moulder G, Barstead R, Tessier-Lavigne M, Bargmann CI (2001) *C. elegans* slit acts in midline, dorsal-ventral, and anterior-posterior guidance via the SAX-3/Robo receptor. Neuron 32:25–38.

Hu H (2001) Cell-surface heparan sulfate is involved in the repulsive guidance activities of Slit2 protein. Nat Neurosci 4:695–701.

Hutson LD, Chien CB (2002) Pathfinding and error correction by retinal axons: the role of astray/robo2. Neuron 33:205–217.

Inatani M, Irie F, Plump AS, Tessier-Lavigne M, Yamaguchi Y (2003) Mammalian brain morphogenesis and midline axon guidance require heparan sulfate. Science 302:1044–1046.

Jones L, López-Bendito G, Gruss P, Stoykova A, Molnar Z (2002) Pax6 is required for the normal development of the forebrain axonal connections. Development 129:5041–5052.

Kidd T, Bland KS, Goodman CS (1999) Slit is the midline repellent for the robo receptor in *Drosophila*. Cell 96:785–794.

Kinnunen A, Niemi M, Kinnunen T, Kaksonen M, Nolo R, Rauvala H (1999) Heparan sulphate and HB-GAM (heparin-binding growth-associated molecule) in the development of the thalamocortical pathway of rat brain. Eur J Neurosci 11:491–502.

Kolodkin AL, Levengood DV, Rowe EG, Tai YT, Giger RJ, Ginty DD (1997) Neuropilin is a semaphorin III receptor. Cell 90:753–762.

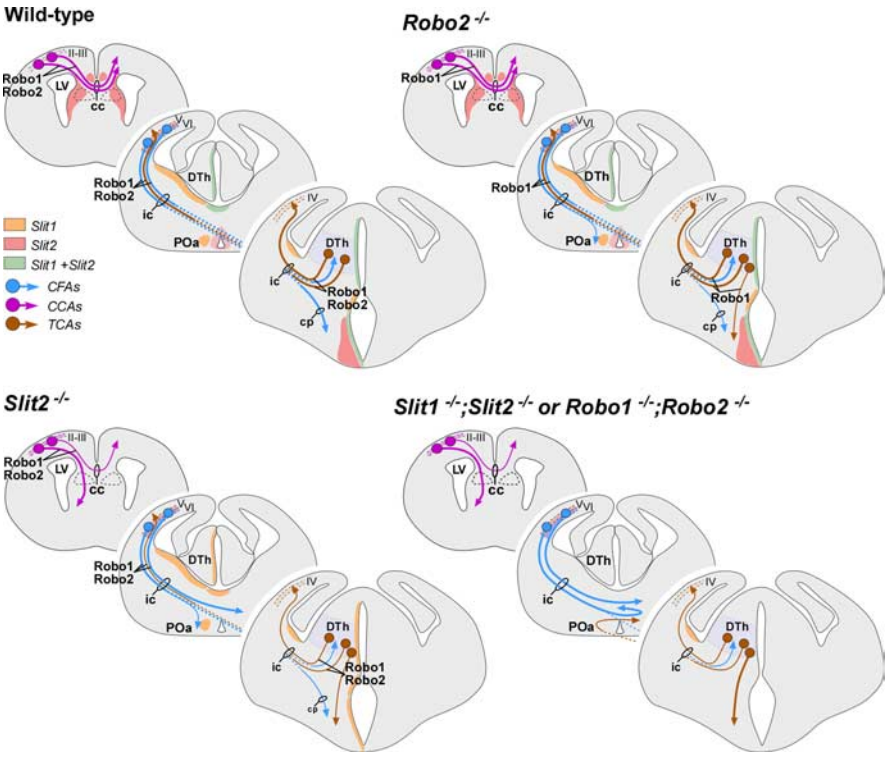

Figure 11. Schematic summarizing axonal defects in the Slit and Robo mutants in relation to regions of Slit action and Robo expression. Slit2 acts in ventral and ventrolateral domains, and Slit1 action is limited to medial areas. In wild-type animals, Slit2 prevents Robo-expressing axons from entering ventral regions and also prevents the axons from coursing medially. Loss of Slit1 does not have an impact on the axonal trajectories because of the continued presence of Slit2. However, loss of Slit2 allows the axons to project ventrally and medially, potentially in response to positive cues from these areas. Mice lacking Robo2 have a less severe phenotype than the one observed in Slit2 $^{-/-}$ because of the presence of Robo1 in those axonal tracts. Only a few corticofugal axons are misrouted from their normal route at the ventral telencephalon. Loss of Robo1 and Robo2 mimics the phenotype observed in mice lacking both Slit1 and Slit2, and allows axons to travel ventrally and medially and to approach and cross the midline. LV, Lateral ventricle; cc, corpus callosum; DTh, dorsal thalamus; ic, internal capsule; cp, cortical plate; VL, ●●●; POa, ●●●.

Lee JS, von der Hardt S, Rusch MA, Stringer SE, Stickney HL, Talbot WS, Geisler R, Nusslein-Volhard C, Selleck SB, Chien CB, Roehl H (2004) Axon sorting in the optic tract requires HSPG synthesis by ext2 (dackel) and extl3 (boxer). Neuron 44:947–960.

Leighton PA, Mitchell KJ, Goodrich LV, Lu X, Pinson K, Scherz P, Skarnes WC, Tessier-Lavigne M (2001) Defining brain wiring patterns and mechanisms through gene trapping in mice. Nature 410:174–179.

Li HS, Chen JH, Wu W, Fagaly T, Zhou L, Yuan W, Dupuis S, Jiang ZH, Nash W, Gick C, Ornitz DM, Wu JY, Rao Y (1999) Vertebrate slit, a secreted ligand for the transmembrane protein roundabout, is a repellent for olfactory bulb axons. Cell 96:807–818.

Liang Y, Annan RS, Carr SA, Popp S, Mevissen M, Margolis RK, Margolis RU (1999) Mammalian homologues of the *Drosophila* slit protein are ligands of the heparan sulfate proteoglycan glypican-1 in brain. J Biol Chem 274:17885–17892.

Long H, Sabatier C, Ma L, Plump A, Yuan W, Ornitz DM, Tamada A, Murakami F, Goodman CS, Tessier-Lavigne M (2004) Conserved roles for Slit and Robo proteins in midline commissural axon guidance. Neuron 42:213–223.

López-Bendito G, Molnár Z (2003) Thalamocortical development: how are we going to get there? Nat Rev Neurosci 4:276–289.

López-Bendito G, Chan CH, Mallamaci A, Parnavelas J, Molnar Z (2002) Role of Emx2 in the development of the reciprocal connectivity between cortex and thalamus. J Comp Neurol 451:153–169.

López-Bendito G, Cautinat A, Sánchez JA, Bielle F, Flames N, Garratt AN, Talmage DA, Role L, Charnay P, Marín O, Garel S (2006) Tangential neuronal migration controls axon guidance: a role for Neuregulin-1 on thalamocortical axon navigation. Cell 125:127–142.

Marillat V, Cases O, Nguyen Ba-Charvet KT, Tessier-Lavigne M, Sotelo C,

Chédotal A (2001) Spatio-temporal expression patterns of slit and robo genes in the rat brain. J Comp Neurol 442:130–155.

McConnell SK, Ghosh A, Shatz CJ (1989) Subplate neurons pioneer the first axon pathway from the cerebral cortex. Science 245:978–982.

Molnár Z, Adams R, Goffinet AM, Blakemore C (1998) The role of the first postmitotic cortical cells in the development of thalamocortical innervation in the reeler mouse. J Neurosci 18:5746–5765.

Métin C, Godement P (1996) The ganglionic eminence may be an intermediate target for corticofugal and thalamocortical axons. J Neurosci 16:3219–3235.

Métin C, Deléglise D, Serafini T, Kennedy TE, Tessier-Lavigne M (1997) A role for netrin-1 in the guidance of cortical efferents. Development 124:5063–5074.

Nguyen Ba-Charvet KT, Brose K, Ma L, Wang KH, Marillat V, Sotelo C, Tessier-Lavigne M, Chedotal A (2001) Diversity and specificity of actions of Slit2 proteolytic fragments in axon guidance. J Neurosci 21:4281–4289.

Nguyen Ba-Charvet KT, Plump AS, Tessier-Lavigne M, Chedotal A (2002) Slit1 and slit2 proteins control the development of the lateral olfactory tract. J Neurosci 22:5473–5480.

Plump AS, Erskine L, Sabatier C, Brose K, Epstein CJ, Goodman CS, Mason CA, Tessier-Lavigne M (2002) Slit1 and Slit2 cooperate to prevent premature midline crossing of retinal axons in the mouse visual system. Neuron 33:219–232.

Price DJ, Kennedy H, Dehay C, Zhou L, Mercier M, Jossin Y, Goffinet AM, Tissir F, Blakey D, Molnar Z (2006) The development of cortical connections. Eur J Neurosci 23:910–920.

Rajagopalan S, Nicolas E, Vivancos V, Berger J, Dickson BJ (2000) Crossing the midline: roles and regulation of Robo receptors. Neuron 28:767–777.

Richards LJ, Koester SE, Tuttle R, O'Leary DD (1997) Directed growth of early cortical axons is influenced by a chemoattractant released from an intermediate target. J Neurosci 17:2445–2458.

Richards LJ, Plachez C, Ren T (2004) Mechanisms regulating the development of the corpus callosum and its agenesis in mouse and human. Clin Genet 66:276–289.

Ronca F, Andersen JS, Paech V, Margolis RU (2001) Characterization of Slit protein interactions with glypican-1. J Biol Chem 276:29141–29147.

Sabatier C, Plump AS, Le M, Brose K, Tamada A, Murakami F, Lee EY, Tessier-Lavigne M (2004) The divergent Robo family protein rig-1/Robo3 is a negative regulator of slit responsiveness required for midline crossing by commissural axons. Cell 117:157–169.

Schaeren-Wiemers N, Gerfin-Moser A (1993) A single protocol to detect transcripts of various types and expression levels in neural tissue and cultured cells: in situ hybridization using digoxigenin-labelled cRNA probes. Histochemistry 100:431–440.

Serafini T, Colamarino SA, Leonardo ED, Wang H, Beddington R, Skarnes WC, Tessier-Lavigne M (1996) Netrin-1 is required for commissural axon guidance in the developing vertebrate nervous system. Cell 87:1001–1014.

Shu T, Richards LJ (2001) Cortical axon guidance by the glial wedge during the development of the corpus callosum. J Neurosci 21:2749–2758.

Shu T, Sundaresan V, McCarthy MM, Richards LJ (2003) Slit2 guides both precrossing and postcrossing callosal axons at the midline in vivo. J Neurosci 23:8176–8184.

Simpson JH, Bland KS, Fetter RD, Goodman CS (2000) Short-range and long-range guidance by Slit and its Robo receptors: a combinatorial code of Robo receptors controls lateral position. Cell 103:1019–1032.

Sundaresan V, Mambetisaeva E, Andrews W, Annan A, Knoll B, Tear G, Bannister L (2004) Dynamic expression patterns of Robo (Robo1 and Robo2) in the developing murine central nervous system. J Comp Neurol 468:467–481.

Torii M, Levitt P (2005) Dissociation of corticothalamic and thalamocortical axon targeting by an EphA7-mediated mechanism. Neuron 48:563–575.

Tuttle R, Nakagawa Y, Johnson JE, O'Leary DD (1999) Defects in thalamocortical axon pathfinding correlate with altered cell domains in Mash-1-deficient mice. Development 126:1903–1916.

Whitford K, Marillat V, Stein E, Goodman C, Tessier-Lavigne M, Chedotal A, Ghosh A (2002) Regulation of cortical dendrite development by Slit-Robo interactions. Neuron 33:47–61.

Yuan W, Zhou L, Chen JH, Wu JY, Rao Y, Ornitz DM (1999) The mouse SLIT family: secreted ligands for ROBO expressed in patterns that suggest a role in morphogenesis and axon guidance. Dev Biol 212:290–306.

Zheng B, Ho C, Li S, Keirstead H, Steward O, Tessier-Lavigne M (2003) Lack of enhanced spinal regeneration in Nogo-deficient mice. Neuron 38:213–224.

AUTHOR QUERIES

AUTHOR PLEASE ANSWER ALL QUERIES 1

A—AU: In affiliation line: Journal style is to spell out acronyms in the affiliation line. Please confirm definitions of CSIC, CNRS, and UMR.

B—AU: Per journal style, 'largely' is changed to 'primarily,' 'mostly,' or 'widely.'

C—AU: Journal style is to spell out the genus name at first use. Please confirm that '*Caenorhabditis*' is correct here.

D—AU: For 'Z. Chen et al., unpublished observations': Please list first/middle initials and last name of each contributor.

E—AU: PFA has been defined at first use in the text. Please confirm definition.

F—AU: Please list affiliation and location (city and state/country) of Fujio Murakami.

G—AU: Journal style is to include both city and state/country with manufacturers at first use. If I knew of a location, I added it. If not correct, please change or delete the location.

H—AU: PB has been defined at first use in the text. Please confirm definition.

I—AU: Molecular Probes is now Invitrogen.

J—AU: NBT and BCIP (each used once in text) have been spelled out. Please confirm definitions.

K—AU: The citation 'Bagri et al., 2001' has been changed to 'Bagri et al., 2002' here to match the reference in the list. Please confirm change.

L—AU: Per journal style, 'due to' has been changed to 'attributable to,' 'caused by,' or 'because of.' Please check throughout and confirm.

M—AU: Is this sentence okay as changed? See sentence beginning 'In contrast to our findings. . . . '

N—AU: In acknowledgments: Journal style is to spell out acronyms in the acknowledgments. Please confirm definitions EURYI, CSIC, FPU, MEC, EMBO, and NARSAD.

O—AU: In correspondence address: CSIC has been spelled out in the correspondence address, per journal style. Please confirm definition.

P—AU: For Figure 1: (1) The abbreviations MPO and VMH do not appear in my copy of this figure. Please check and delete definitions of these abbreviations, if necessary. (2) Please define POa (used in panels *A* and *D*).

AUTHOR QUERIES

AUTHOR PLEASE ANSWER ALL QUERIES 2

Q—AU: For Figure 2: The abbreviation HC does not appear in my copy of this figure. Please check and delete definition of this abbreviation, if necessary.

R—AU: For Figure 3: Please describe the asterisk in panel *D*.

S—AU: For Figure 5: (1) My copy of this figure does not show the abbreviation LA. Please check and delete abbreviation and definition from legend, if necessary. (2) Please confirm definition of the abbreviation 'H' (inserted in legend).

T—AU: For Figure 8: Please confirm definitions of GP and H (inserted in legend).

U—AU: For Figure 10: Please define CM and VL (used in panels *A* and *B*).

V—AU: For Figure 11: (1) Please confirm definitions of LV, cc, DTh, ic, and cp (inserted in legend). (2) Please define VL and POa.